Ordered-defect sulfides as thermoelectric materials

Article

Accepted Version

Ordered-defect sulphides as thermoelectric materials

Andreas Kaltzoglou[1,3], Paz Vaqueiro[1,3], Tristan Barbier[2], Emmanuel Guilmeau[2], Anthony V. Powell[1,3,*]

[1] *Institute of Chemical Sciences, Heriot-Watt University, Edinburgh EH14 4AS,* United Kingdom
[2] *Laboratoire CRISMAT, UMR 6508 CNRS/ENSICAEN, 6 bd du Maréchal Juin, F-14050 CAEN Cedex 4, France*
[3] *Present address: Department of Chemistry, University of Reading, Whiteknights, Reading RG6 6AD, United Kingdom*

* Corresponding author: a.v.powell@reading.ac.uk

The thermoelectric behaviour of the transition-metal disulphides *n*-type $NiCr_2S_4$ and *p*-type $CuCrS_2$ is investigated. Materials prepared by high-temperature reaction were consolidated using cold-pressing and sintering, hot-pressing (HP) in graphite dies or spark-plasma sintering (SPS) in tungsten carbide dies. The consolidation conditions have a marked influence on the electrical transport properties. In addition to the effect on sample density, altering the consolidation conditions results in changes to the sample composition, including the formation of impurity phases. Maximum room-temperature power factors are 0.18 mW m^{-1} K^{-2} and 0.09 mW m^{-1} K^{-2} for $NiCr_2S_4$ and $CuCrS_2$, respectively. Thermal conductivities of *ca.* 1.4 and 1.2 W m^{-1} K^{-1} lead to figures of merit of 0.024 and 0.023 for $NiCr_2S_4$ and $CuCrS_2$, respectively.

Keywords *Thermoelectric properties, transition metal sulphides, hot pressing, spark plasma sintering, consolidation methods*

Introduction

Thermoelectric materials are of increasing interest for applications involving energy harvesting from waste heat. The efficiency of a thermoelectric device is dependent on the physical properties of the component materials. In particular, the thermoelectric performance of a material is dependent on an unusual combination of high electrical conductivity (σ), typically found in metals, together with a low thermal conductivity (κ) and high Seebeck coefficient (S), characteristics more usually associated with non-metallic systems, and is embodied in the dimensionless figure of merit, $ZT = S^2\sigma T/\kappa$ [1]. Recently, there has been renewed interest in sulphide-based

thermoelectrics and the potential they offer for low-cost alternatives to the current commercial material of choice, Bi_2Te_3.

In the search for sulphide-based thermoelectrics, we have recently begun to investigate the potential of ordered-defect phases. These materials comprise two-dimensional dichalcogenide slabs of edge-sharing octahedra stacked in a direction perpendicular to the slab direction. The van der Waals' gap between adjacent slabs consists of a network of vacant octahedral and tetrahedral sites. Partial occupancy of such sites by cations in phases, A_xMS_2, may occur in an ordered fashion giving rises to a range of two-dimensional superstructures [2], some of which are stable over a range of x. The nature of the cation ordering is also temperature dependent and order-disorder transitions are commonly observed at elevated temperatures [3,4,5]. Ordered-defect phases are attractive candidates for thermoelectrics as they combine low-dimensionality, intrinsic to the dichalcogenide slab, with the capacity to tune electron-transport properties through chemical substitution. For example, substitution of vanadium for chromium in $NiCr_2S_4$ ($Ni_{0.5}CrS_2$) effects a semiconductor to metal transition at a critical level of substitution, $x_c \approx 0.4$ [6,7].

Here, we present a preliminary investigation of the thermoelectric properties of $NiCr_2S_4$ and $CuCrS_2$ which each contain CrS_2 slabs. The former adopts a monoclinic structure at room temperature [8] in which 50% of the octahedral sites between pairs of dichalcogenide slabs are occupied by cations (Fig 1(a)). At room temperature $CuCrS_2$ adopts a trigonal structure [9] in which 50% of tetrahedral sites are occupied between pairs of CrS_2 slabs (Fig 1(b)). Our previous measurements of the electrical transport properties of cold-pressed and sintered samples of $NiCr_2S_4$ reveal *n*-type semiconducting behavior and lead to determination of the thermoelectric power factor as *ca.* 0.1 mW m^{-1} K^{-2} at room temperature [10]. However, to the best of our knowledge, the thermal conductivity of this phase has not been determined. The thermoelectric properties of *p*-type $CuCrS_2$ have been the subject of considerable recent interest following the report of a figure of merit as high as 2.0 at room temperature [11,12]. The performance of this material appears to be sensitive to the thermal history of the sample. Extended sintering at high temperatures (850 – 900 °C) followed by quenching in air appears to be required for optimum properties, as it promotes copper-ion disorder, thereby reducing the thermal conductivity, and leads to increased texture of the sample, which increases the electrical conductivity. However, recent work by another group has shown that SPS processed samples exhibit a much higher electrical resistivity than previously reported and the maximum figure of merit, $ZT = 0.11$, is

observed at 400 °C [13]. At higher temperatures volatilization of sulphur was observed leading to a reduced charge-carrier concentration and a transition from *p*- to *n*-type conductivity.

In this work, we describe an investigation of the impact of the consolidation method on the thermoelectric properties of $NiCr_2S_4$ and $CuCrS_2$. The results demonstrate that the consolidation method has a marked effect on materials' properties through grain growth, which manifests itself in differences in the degree of densification and through changes in the chemical composition of the sample, including the formation of impurity phases, which can produce variations in the electrical transport properties by up to an order of magnitude and even induce a change in the dominant charge carriers from electrons to holes.

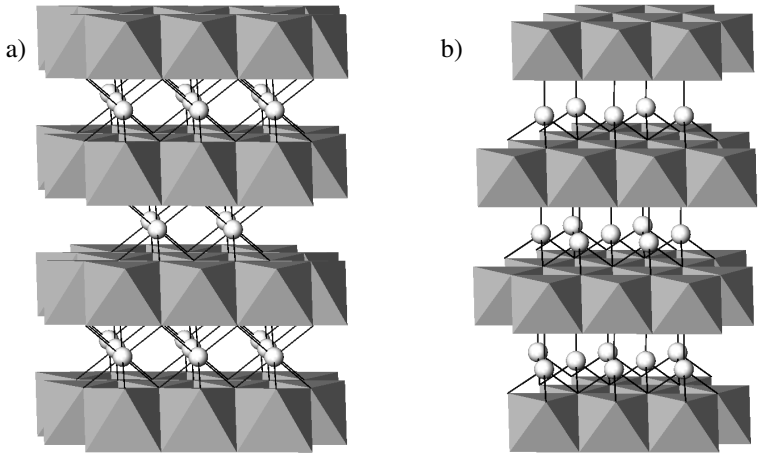

Fig.1 Crystal structure of a) $NiCr_2S_4$ and b) $CuCrS_2$ with Ni and Cu atoms (open circles) partially filling octahedral and tetrahedral gaps, respectively, between edge-sharing CrS_6 octahedra (grey).

Experimental

Materials were synthesized by reaction of appropriate mixtures of the elements (Ni (Aldrich, 99.9%), Cu (Aldrich, 99.5%), Cr (Aldrich, 99+%) and S (Aldrich, 99.99+%)) at high temperatures in evacuated (< 10^{-4} Torr) silica tubes. In the case of the nickel-containing phase, a reaction mixture slightly deficient in sulphur was used, corresponding to a composition, $NiCr_2S_{3.93}$, whereas that for the copper-containing materials the reaction mixture was stoichiometric. $NiCr_2S_4$ was heated at 900 °C for 1 day before annealing at 500 °C for 5 hours whilst $CuCrS_2$ was heated at 500 °C for 12 hours. $CuCrS_2$ was also synthesised by mechanical alloying (MA) in a PM100 Retsch planetary ball mill, using a steel jar and grinding balls at 650 rpm for 24 hours. Powder X-ray diffraction data for all materials were collected using a Bruker D8 Advance powder diffractometer, operating with Ge-monochromated Cu $K_{\alpha 1}$ radiation (λ = 1.5406 Å) and equipped

with a LynxEye linear detector. Rietveld refinements were performed using the GSAS software package [14].

With the exception of one batch of $NiCr_2S_4$ that was micronized by ball milling (1h at 400 rpm) and the sample of $CuCrS_2$ made by mechanical alloying, all materials were ground to a fine powder in an agate mortar prior to consolidation. Powdered samples were consolidated by cold-pressing at 750 MPa in a stainless steel die followed by sintering for four days at 800 °C in an evacuated sealed silica; by hot-pressing (HP) in graphite die for 30 minutes under a N_2 atmosphere at various temperatures and pressures; and by spark-plasma sintering (SPS) on an FCT instrument using tungsten carbide dies under 300 MPa and at various temperatures. Details of temperatures and pressures are provided in the results section. Sulphur analysis for selected samples was carried out by inductively coupled plasma–atomic emission spectroscopy (Exeter Analytical (UK)).

Rectangular ingots with approximate dimensions of $2 \times 2 \times 10$ mm^3 were cut from the compacted pellets and polished with fine sandpaper. The electrical resistivity (4-probe DC) and Seebeck coefficient of the ingots were determined over the temperature range $40 \leq T/°C \leq 300$ under a static He atmosphere of 1.1 – 1.4 bar using a Linseis LSR-3 instrument. Corresponding data for $NiCr_2S_4$ consolidated by SPS were obtained over the temperature range $30 \leq T/°C \leq 300$ using an Ulvac ZEM-3 instrument. The thermal conductivity of $NiCr_2S_4$ at room temperature was measured using a TPS 2500s instrument, whereas that of $CuCrS_2$ was determined using a Quantum Design Physical Property Measurement System.

Results and Discussion

Materials characterization

Rietveld analysis of powder X-ray diffraction data confirms that all reaction products are phase pure materials. Powder diffraction data for $NiCr_2S_4$ are well described (Fig. 2) by a monoclinic structural model involving complete ordering of Ni and Cr over octahedral sites. It was not possible to refine the sulphur content, owing to the small deviation from stoichiometry. Rietveld refinement using powder X-ray diffraction data collected for $CuCrS_2$ (Fig. 3), reveals that Cu and Cr atoms are fully ordered in tetrahedral and octahedral sites respectively.

The density of the consolidated samples of $NiCr_2S_4$ increases with increasing consolidation temperature and pressure (Table 1), reaching *ca*. 99% of the crystallographic density when

processed by SPS (650 °C, 300 MPa). Notably, powder X-ray diffraction data for consolidated samples reveals *ca.* 5 wt% of NiS_2 impurity in the samples consolidated by HP at 100 MPa and by SPS at 300 MPa. The presence of NiS_2 is consistent with an increased sulphur content determined by elemental analysis of the sample processed by HP at 100 MPa. The absence of any chromium-containing decomposition products in powder X-ray diffraction data suggests that this phase can tolerate a degree of non-stoichiometry on the nickel and sulphur sub-lattices. The sample processed by HP at 600 °C, 60 MPa exhibits a sulphur content slightly lower than that expected from the reaction stoichiometry, suggesting some volatilization may occur under these conditions.

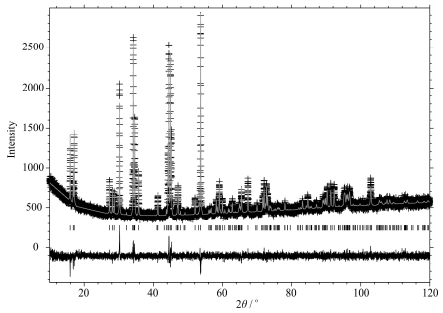

Fig. 2 Final observed (crosses), calculated (solid line) and difference (full lower line) profiles from Rietveld refinements for $NiCr_2S_4$ using powder X-ray diffraction data (Space group: *I2/m*, a = 5.91128(8), b = 3.41042(5), c = 11.1094(1) Å, β = 91.163(1)º; R_{wp} = 4.90%, χ^2 = 1.26)

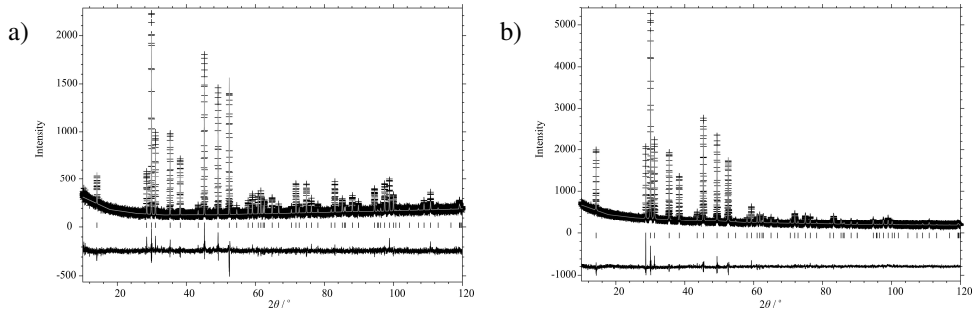

Fig. 3 Final observed (crosses), calculated (solid line) and difference (full lower line) profiles from Rietveld refinements for (a) as-synthesized $CuCrS_2$ using powder X-ray diffraction data. (Space Group: *R*3, a = 3.47962(2) Å, c = 18.6927(2) Å, R_{wp} = 8.63%, χ^2 = 1.37) and (b) for cold-pressed and sintered $CuCrS_2$ illustrating the change in reflection intensities due to texturing. (Space Group: *R*3, a = 3.48038(3) Å, c = 18.6969(2) Å, R_{wp} = 7.36%, χ^2 = 1.63)

The density of the consolidated samples of $CuCrS_2$ ranges from 89% to 97% of the crystallographic value (Table 2). Under the same hot-pressing conditions, the density of the MA sample is slightly higher than for the sample obtained by conventional reaction. Powder X-ray diffraction indicates no sample decomposition occurs under any of the consolidation conditions investigated. However, powder X-ray diffraction data for the sample produced by cold-pressing exhibit a marked increase in the intensity of (00*l*) reflections (Fig. 3 (b)), suggesting preferred

orientation due to texturing. This is consistent with previous reports [11], which suggest that texturing occurs on prolonged high-temperature sintering followed by fast quenching of the polycrystalline solid.

Table 1. Consolidation conditions and bulk characteristics for $NiCr_2S_4$ samples.

Consolidation conditions	Code	Density[2] (g cm^{-3})	S content[3] (wt%)	Impurity phases
HP at 600 °C / 60 MPa	1a	3.31	43.52	None detected
HP at 600 °C / 110 MPa	2a	3.61	45.15	NiS_2
HP at 600 °C / 60 MPa[1]	3a	3.16	—	None detected
HP at 680 °C / 60 MPa	4a	3.68	—	None detected
HP at 800 °C / 60 MPa	5a	3.72	—	None detected
SPS at 600 °C / 300 MPa	6a	4.18	—	NiS_2 detected
SPS at 650 °C / 300 MPa	7a	4.27	—	NiS_2 detected

[1] Powder ball milling at 400 rpm for 1 hour prior to hot pressing
[2] Crystallographic density: d = 4.31 g cm^{-3}
[3] 43.65 wt% S content expected for $NiCr_2S_{3.93}$ and 44.08 wt% for $NiCr_2S_4$

Table 2. Consolidation conditions and density for $CuCrS_2$ samples.

Consolidation conditions	Code	Density[2] (g cm^{-3})
Cold pressing at 700 MPa, sintered 4d at 850 °C quenched	1b	4.06
Hot pressing at 600 °C, 60 MPa	2b	4.15
Hot pressing at 600 °C, 60 MPa[1]	3b	4.23
Hot pressing at 650 °C, 100 MPa	4b	4.44

[1] Obtained by mechanical alloying
[2] Crystallographic density: d = 4.56 g cm^{-3}

Physical properties

The electrical resistivity and Seebeck coefficient data for $NiCr_2S_4$ (Fig. 4) reveal a marked dependence of the electrical transport properties on the consolidation method. Whilst electrons are the dominant charge carriers in all consolidated materials, the resistivity of HP samples changes from a semiconducting to a metallic-like temperature dependence with increasing density, whereas the two SPS processed samples exhibit semiconducting behaviour. The Seebeck coefficient at 40 °C ranges from -18 to -172 μV K^{-1} depending on the processing method. For the SPS processed samples, the absolute value of the Seebeck coefficient decreases with increasing temperature, whereas for most of the hot-pressed samples Seebeck coefficient increases in absolute value with increasing temperature. The temperature dependence of the electrical resistivity and the Seebeck coefficient of the hot-pressed samples is characteristic of conduction by extrinsic charge carriers, and indicate that these samples behave as degenerate semiconductors. The highest power factor of 0.18 mW m^{-1} K^{-2} at room temperature is reached for the material processed by SPS at 650 °C, 300

MPa and is higher than that determined in our previous report on cold-pressed and sintered pellets [10]. The difference may be attributed to the lower relative density (*ca.* 75%) of the latter material, which leads to an increase in the electrical resistance (by a factor of 2) over the SPS processed sample. The thermal conductivity of $NiCr_2S_4$ processed by HP at 680 °C, 60 MPa was determined as 1.4 W m^{-1} K^{-1} at 40 °C, leading to a figure of merit, $ZT \approx 0.024$.

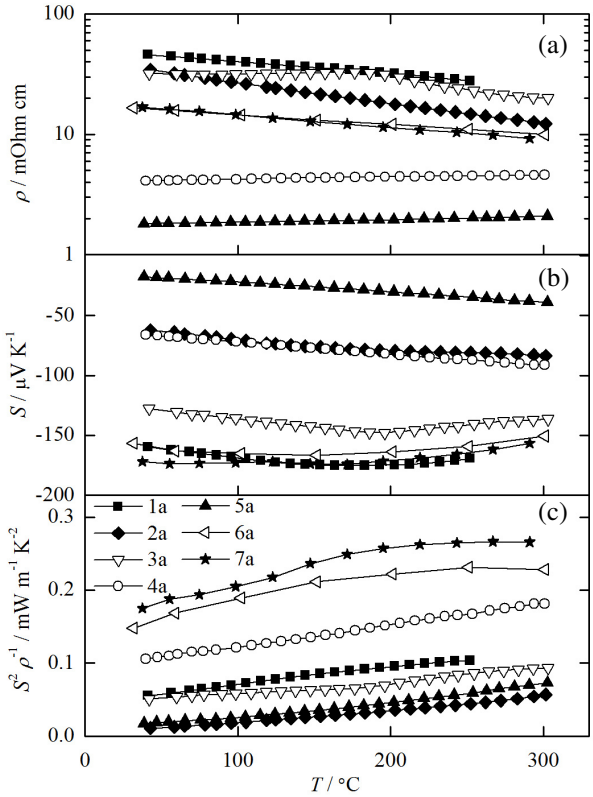

Fig. 4 Thermoelectric properties of $NiCr_2S_4$ over the temperature range $30 \leq T$ / °C ≤ 300 (a) electrical resistivity in logarithmic scale (b) Seebeck coefficient and (c) power factor.

All consolidated samples of $CuCrS_2$ behave as *p*-type semiconductors (Fig. 5). The Seebeck coefficient of HP samples, show an almost linear increase with temperature whereas in the cold-pressed and sintered sample the value is almost temperature independent. In the latter case, a power factor of 0.09 mW m^{-1} K^{-2} and thermal conductivity measured as κ(40 °C) ≈ 1.2 W m^{-1} K^{-1} lead to $ZT \approx 0.023$ at room temperature. This performance is much lower than that in the original report by Tewari *et al* (ρ = 6 mOhm cm, S = 445 μV K^{-1}, κ = 0.48 W m^{-1} K^{-1} and ZT = 2 at room temperature) [11] but is in good agreement with a large number of literature reports on the thermoelectric properties of this phase [13,15,16,17]. The principal origin of the discrepancy is believed to be the strong anisotropy in the cold-pressed and sintered sample [9]. The bond strength between Cu cations in the van der Waals' gap and S anions in the CrS_2 slabs has a significant

effect on the Cu^+ ionic conductivity [18]. The increase in unit cell volume upon prolonged sintering, observed here [19] and in a previous study where the *c* parameter increases upon sintering at 900˚C for 8 days [9], may be indicative of a weakening of this bonding and increased mobility of Cu^+ species. The formation on consolidation of point defects associated with the copper ion sub-lattice, may also influence the electrical properties [20], although if present, these are at too low a level to be detected in Rietveld refinement using powder X-ray diffraction data.

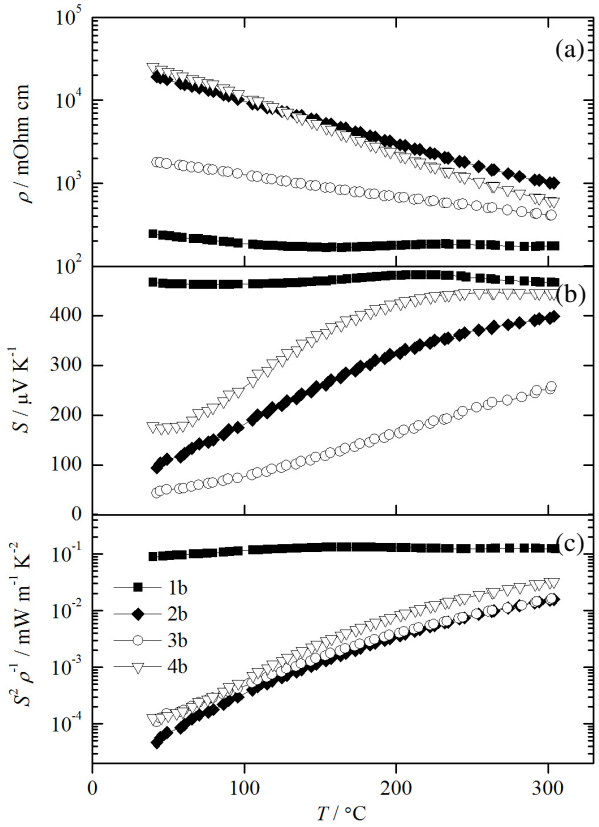

Fig. 5 Thermoelectric properties of $CuCrS_2$ over the temperature range $40 \leq T / {}^{o}C \leq 300$ (a) electrical resistivity in logarithmic scale (b) Seebeck coefficient and (c) power factor.

Conclusions

Both $NiCr_2S_4$ and $CuCrS_2$ exhibit a modest thermoelectric response. The highest measured power factor of 0.27 mW m^{-1} K^{-2} at 267 °C for the SPS-processed sample of $NiCr_2S_4$ is considerably lower than for the best *n*-type materials such as the skutterudite $Yb_{0.19}Co_4Sb_{12}$ [21, 22], which exhibits a power factor of up to 4 mW m^{-1} K^{-2} at 300 °C. However, there is considerable scope for tuning the thermoelectric properties of ordered-defect phases through chemical substitution, to which such materials are particularly amenable. The work reported here

also demonstrates that the consolidation process may have a marked effect on the thermoelectric properties of $NiCr_2S_4$ and $CuCrS_2$. Variations in electron-transport properties of up to an order of magnitude are observed depending on the consolidation conditions used. In addition to changes in sample composition that are evidenced by powder X-ray diffraction, variations in sample density occur. These are likely to reflect changes in the microstructure of the materials involving differences in grain growth and grain boundary formation. Detailed examination by microscopy techniques are required to characterise such changes at the microstructural level.

Acknowledgements

Financial support by the European Commission (FP7-SME-2012-1, Grant Agreement no. 315019) is gratefully acknowledged. We wish to thank Drs. Lars Hälldahl, K-Analys AB, Sweden and Ramzy Daou, Laboratoire CRISMAT, France for thermal conductivity measurements.

References

[1] J.R. Sootsman, D.Y. Chung, M.G. Kanatzidis, Angew. Chem. Inter. Ed. 48, 8616 (2009)

[2] P. Vaqueiro, A.V. Powell, Chem. Mater. 12, 2705 (2000)

[3] P. Vaqueiro, S. Hull, B. Lebech, A.V. Powell, J. Mater. Chem. 9, 2859 (1999)

[4] P. Vaqueiro, A.V. Powell, B. Lebech, Physica B 276, 238 (2000)

[5] I.G. Vassilieva, T.Yu. Kardash, V.V. Malakhov, J. Struct. Chem. 50, 288 (2009)

[6] R.J. Bouchard, A Wold, J. Phys. Chem. Solids 27, 591 (1966)

[7] A.V. Powell, P. Vaqueiro, A. McDowall, Solid State Ionics 172, 469 (2004)

[8] A.V. Powell, D.C. Colgan, C. Ritter, J. Solid State Chem. 134, 110 (1997)

[9] G.C. Tewari, T.S. Tripathi, A.K. Rastogi, Z. Kristallogr. 225, 471 (2010)

[10] A.V. Powell, P. Vaqueiro, T. Ohtani, Phys. Rev. B 71, 125120 (2005)

[11] G.C. Tewari, T.S. Tripathi, A.K. Rastogi, J. Elec. Mat. 39, 1133 (2010)

[12] G.C. Tewari, T.S. Tripathi, P. Kumar, A.K. Rastogi, S.K. Pasha, G. Gupta, J. Elec. Mat. 40, 2368 (2011)

[13] Y.-X. Chen, B.-P. Zhang, Z.-H. Ge, P.-P. Shang, J. Solid State Chem. 186, 109 (2012)

[14] A.C. Larson, R.B. von Dreele, General Structure Analysis System, Los Alamos Laboratory, [Report LAUR 85-748] (1994)

[15] C-G Han, B-P Zhang, Z-H Ge, L-J Zhang, Y-C Liu, J. Mater. Sci. 48, 4081 (2013)

[16] G.M. Abramova, A.M. Vorotynov, G.A. Petrakovskii, N.I. Kiselev, D.A. Velikanov, A.F. Bovina, R.F. Al'mukhametov, R.A. Yakshibaev, É.V. Gabitov, Phys. Solid State 46, 2225 (2004)

[17] N. Le Nagard, G. Collin, O. Gorochov, Mat. Res. Bull. 14, 1411 (1979)

[18] R.F. Almukhametov, R.A. Yakshibayev, E.V. Gabitov, A.R. Abdullin, R.M. Kutusheva, Phys. Stat. Sol. (b) 236, 29 (2003)

[19] The lattice parameters increase from a = 3.47962(2) Å, c = 18.6927(2) for an as-synthesised sample to a = 3.48038(3) Å, c = 18.6969(2) Å for a cold-pressed and sintered sample.

[20] M.A. Boutbila, J. Rasneur, M.E. Aatmani, J. Alloys Comp. 283, 88 (1999)

[21] G.S. Nolas, M. Kaeser, R.T. Littleton, T.M. Tritt, Appl. Phys. Lett. 77, 1855 (2000)

[22] J. Garcia-Canadas, A.V. Powell, A. Kaltzoglou, P. Vaqueiro, G. Min, J. Elec. Mat. 42, 1369 (2013)